Electrochemical Study of Anionic Ferrocene Derivatives Intercalated in Layered Double Hydroxides: Application to Glucose Amperometric Biosensors

ARTICLE *in* ELECTROANALYSIS · FEBRUARY 2009

Impact Factor: 2.14 · DOI: 10.1002/elan.200804407

4 AUTHORS:

Christine Mousty
Université Blaise Pascal - Clermont-Ferrand II
116 PUBLICATIONS **2,385** CITATIONS
SEE PROFILE

Claude Forano
Blas Pascal University
132 PUBLICATIONS **2,669** CITATIONS
SEE PROFILE

Solenne Fleutot
University of Lorraine
17 PUBLICATIONS **240** CITATIONS
SEE PROFILE

Jean-Charles Dupin
Université de Pau et des Pays de l'Adour
44 PUBLICATIONS **1,089** CITATIONS
SEE PROFILE

Full Paper

Electrochemical Study of Anionic Ferrocene Derivatives Intercalated in Layered Double Hydroxides: Application to Glucose Amperometric Biosensors

Christine Mousty,[a]* *Claude Forano*,[a] *Solenne Fleutot*,[b] *Jean-Charles Dupin*[b]

[a] Laboratoire des Matériaux Inorganiques, Université Blaise Pascal – CNRS UMR 6002 FR 2404, 24 Av des Landais, 63177 Aubière Cedex, France
[b] IPREM – CNRS UMR 5254, Hélioparc, 2 Av. du Président Angot, 64053 Pau Cedex9, France
*e-mail: Christine.Mousty@univ-bpclermont.fr

Received: July 15, 2008
Accepted: September 16, 2008

Abstract
Layered double hydroxides ($Zn_2Cr(OH)_6X \cdot nH_2O$ LDH) containing (3-sulfopropyl)ferrocene-carboxylate ($FcPSO_3$) and 1,1′-bis(3-sulfopropyl)ferrocene-carboxylate ($Fc(PSO_3)_2$) as interlayer anions (X) have been prepared by the co-precipitation method and characterized by PXRD, FTIR, SEM and XPS. The electrochemical behavior of these hybrid materials has been evaluated by cyclic voltammetry. A new amperometric biosensor based on the immobilization of glucose oxidase in ZnCr-$FcPSO_3$ hybrid material was presented, the intercalated anions playing the role of mediators that shuttle electrons between the FAD centers in the enzyme and the electrode surface. The performance of the resulting biosensor for glucose determination under anaerobic conditions was evaluated by chronoamperometry at 0.5 V. The sensitivity (65 mA M^{-1} cm^{-2}) determined in the concentration range 10 – 25 μM is higher than sensitivities reported for other glucose biosensors based on LDH host matrices.

Keywords: Layered double hydroxides, Ferrocene derivatives, Glucose oxidase, Biosensor

DOI: 10.1002/elan.200804407

1. Introduction

Inorganic-organic hybrid materials are specially tailored to give desirable multifonctionnalities in which a synergic effect of specific properties of both components is expressed. For example, sensing applications require materials with transducer properties and biosensing applications require additionally materials providing a protective environment for the biomolecule that preserves its bioactivity [1]. The most common types of hybrid materials used for analytical applications include the sol-gel materials [2, 3] and the layered compounds such as clays [4].

The hybrid layered compounds result from the intracrystalline insertion of organic molecules or biomolecules between the layers of lamellar solids [5]. For example, layered double hydroxides (LDH), also referred as anionic clays or hydrotalcite like compounds, are solids showing 2D structural arrangement with the general formula $[M^{II}_{1-X}M^{III}_X(OH)_2]^{x+}[X^{q-}_{x/q} \cdot nH_2O]$ (abbreviated as $M^{II}M^{III}$-X). Due to their unique anionic exchange properties LDH are very appropriate materials for the immobilization organic anions and biomolecules that often bear an overall negative charge [6, 7]. One of the most promising application field of LDH is their use as host structure for enzymes for the development of biosensors [8, 9]. Various soft chemistry processes such as adsorption, delamination/restacking, chemical grafting, co-precipitation and electrodeposition methods have been used to synthesize these new active bioinorganic LDH-Enzyme nanohybrid materials [9 – 11].

On the other hand, we have published several years ago structural and electrochemical characterizations of hybrid LDH containing organic electroactive molecules bearing an anionic group such as nitrobenzene sulfonate, anthraquinone mono and disulfonate [12], 2,2′-azinobis 3-ethylbenzothiazoline-6-sulfonate (ABTS) [13], nitroxide and ferrocene mono and disulfonate ($FcSO_3$, $Fc(SO_3)_2$) [14, 15]. More recently, other laboratories have reported on the confinement of electroactive molecules within LDH structures, in particular ferrocene derivatives. Different immobilization strategies have been adopted depending on the ferrocene moieties. Ferrocenesulfonate, ferrocenecarboxylate, ferrocenebutyrate anions were intercalated by the co-precipitation method between the LDH layers with different compositions, namely ZnCr, ZnAl and MgAl [14 – 17]. Neutral ferrocene or ferrocene methanol were immobilized receptively by inclusion within cyclodextrin cavities grafted into LDH [18] or by simple adsorption on the LDH particles [19]. Modified electrodes using ferrocene carboxylate confined on surfactant-LDH have been applied to the electrocatalytic oxidation of ascorbic acid, uric acid [20] and nicotinamide adenine dinucleotide (NADH) [21]. Very recently, LDH containing ferrocene derivatives have been used as immobilization matrix of glucose oxidase (GOx) for the development of amperometric biosensors [19, 22].

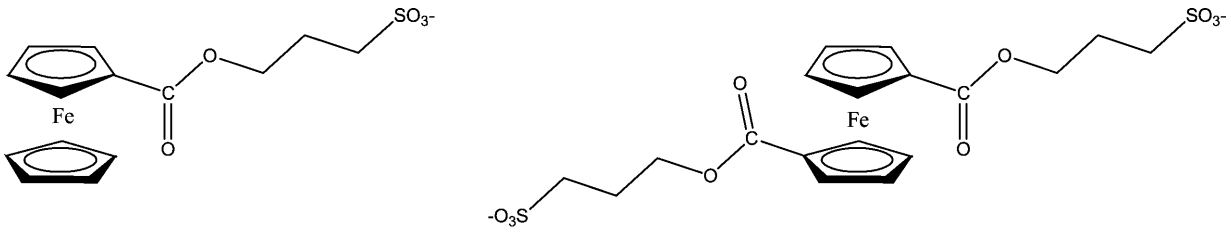

$FcPSO_3$ **$Fc(PSO_3)_2$**

Fig. 1. Structural formula of $FcPSO_3^-$ and $Fc(PSO_3)_2^{2-}$.

Indeed, ferrocene and derivatives are the most widely used class of mediators in the fabrication of stable and sensitive biosensors [23]. A number of cases has been reported where glucose oxidase and ferrocene derivatives both are immobilized at the electrode surface leading to heterogeneous electron transfer. Besides conducting polymers with grafted ferrocene units [24], various inorganic materials, such as ormosil [25], sono-gel [26], titanium oxide [27], and vanadium pentoxide xerogel [28] have also been used as immobilization matrices for the fabrication of mediated glucose biosensors.

In the present work, new nanohybrid LDH containing ferrocene anions ($FcPSO_3$ and $Fc(PSO_3)_2$, Fig. 1) were synthesized by the co-precipitation method and characterized by XRD, FTIR, SEM, XPS and electrochemistry. The resulting ZnCr-$FcPSO_3$ hybrid material was used for the immobilization of GOx and applied to the detection of glucose under anaerobic condition. Finally analytical characteristics of different glucose biosensors based on LDH matrices are examined in relation to their different compositions.

2. Experimental

2.1. Chemicals

1,2-propane sultone, ferrocenecarboxylic acid, 1,1′-ferrocenedicarboxylic acid, glucose oxidase (269 U/mg) were purchased from Aldrich. Zinc chloride and chromium chloride are Prolabo products. All other reagents were of analytical grade. All solutions were prepared with decarbonated water.

Ferrocene esters $FcPSO_3$ and $Fe(PSO_3)_2$ were synthesized using the propane sultone as sulfoalkylating agent [29]. The reaction between 500 mg (1.98 mmol) ferrocene carboxylate sodium salt and 200 μL (2.20 mmol) 1,3 propane sultone was carried out in the solid phase at 140 °C for 4 h. The solid product was washed with ether and purified by column chromatography on silica gel (chloroform-methanol 70/30, $R_f = 0.39$). 350 mg (70%) $FcPSO_3$ was obtained: ^{1}H NMR (Brucker MDL 400 MHz in DMSO-d_6) δ 2.00 (q, 2H); 2.60 (t, 2H); 4.25 (t, 2H); 4.25 (s, 5H), 4.50 (s, 2H); 4,80 (s,2H) ppm. The same protocol was used for $Fc(PSO_3)_2$, starting with 700 mg 1,1′-ferrocenedicarboxylate sodium salt and 463 μL (5.28 mmol) 1,3 propane sultone. The reaction was stopped after 24 h and the product was purified by chromatography on silica gel (chloroform-methanol 60/40, $R_f = 0.36$). 464 mg (46 %) of $Fc(PSO_3)_2$ was obtained: ^{1}H NMR (Brucker MDL 400 MHz in DMSO-d_6) δ 2.00 (q, 4H); 2.60 (t, 4H); 4.25 (t, 4H); 4.55 (s, 4H), 4,80 (s,4H) ppm.

ZnCr-$FcPSO_3$ and ZnCr-$Fc(PSO_3)_2$ LDH were prepared by co-precipitation as follows: an aqueous solution containing 20 mmol $ZnCl_2$ and 10 mmol $CrCl_3 \cdot 6H_2O$ was added dropwise to a stirred solution (20 mL) of decarbonated water containing two equivalents in charge of ferrocene derivatives per mol of chromium· over a period of 24 h. The solution was maintained under nitrogen atmosphere in order to minimize the contamination with atmospheric CO_2. A solution of sodium hydroxide (1 M) was simultaneously added by means of a pH regulator with a pH electrode immersed in the reagent solution to fix the pH of co-precipitation at 5.0. The precipitate was separated by centrifugation, washed with deionized water and dried at room temperature. The ZnCr-Cl reference material was co-precipitated at pH 6.5 in anion free deionized water following similar conditions. Chemical formulae are respectively $Zn_2Cr(OH)_6.Fe(C_{14}H_{15}SO_5) \cdot nH_2O$ (ZnCr-$FcPSO_3$), $Zn_2Cr(OH)_6.[Fe(C_{18}H_{20}S_2O_{10})]_{0.5} \cdot nH_2O$ (ZnCr-$Fc(PSO_3)_2$) and $Zn_2Cr(OH)_6.Cl \cdot nH_2O$ (ZnCr-Cl).

2.2. Apparatus

ZnCr-$FcPSO_3$ and ZnCr-$Fc(PSO_3)_2$ LDH were characterized by PXRD, FTIR, SEM and XPS. Powder X-ray diffraction patterns were recorded on a Siemens D501 diffractometer using CuKα radiation. Patterns were recorded over the 2.0 – 70 2θ range in steps of 0.04° with a counting time per step of 75 s and over the 1 – 10 2θ range in steps of 0.04° with a counting time per step of 16 s. Transmission FTIR (KBr pellet) spectra were recorded on a Nicolet 5700 (Thermo electron corporation) spectrometer The size of particles were measured by photocorellation spectroscopy with the Zetasizer nanoZS Malvern instrument and the scanning electron micrographs (SEM) of LDH samples were recorded on a Zeiss supra 55-VP microscope at an electron energy of 2 kV.

XPS analyses were performed on a Kratos Axis Ultra photoelectron spectrometer which employed a magnetic

immersion lens to increase the solid angle of photoelectrons collection from small analysis areas to minimize the aberrations of the electron optics. A monochromatic and focused (spot dimensions of 700 μm by 300 μm) Al K_α radiation (1486.6 eV) was operated at 450 W under a residual pressure of 5×10^{-9} mbar. The spectrometer was calibrated using the photoemission lines of Au ($Au4f_{7/2} =$ 83.9 eV, with reference to the Fermi level) and Cu ($Cu2p_{3/2} = 932.5$ eV); for the $Au4f_{7/2}$ line, the full width at half maximum (FWHM) was 0.86 eV in the recording conditions. Charge effects were compensated by the use of a charge neutralization system (low energy electrons [typically 1.85 eV]) which had the unique ability to provide consistent charge compensation. All the neutralizer parameters remained constant during analysis. Peaks were then shifted to align adventitious hydrocarbon C1s photoemission to 284.6 eV binding energy. High resolution regions were acquired at a constant pass energy of 40 eV. The XPS signals were analyzed by using a least squares algorithm and a nonlinear baseline. The fitting peaks of the experimental curves were defined by a combination of Gaussian (70%) and Lorentzian (30%) distributions. All the samples were grinded prior to analysis to avoid effects due to the surface texture.

2.3. Electrochemical Procedures

LDH modified electrodes were prepared as a film on a glassy carbon electrode with a diameter of 3 mm for cyclic voltammetry and 5 mm under rotation conditions (500 rpm) for batch chronoamperometric experiments. Before use, the glassy carbon electrodes were polished with 1 μM diamond paste and rinsed with ethanol, acetone and distilled water. Hybrid LDH suspensions (4 mg/mL) was stirred at least overnight before use. Aliquots (20 – 40 μL) of ZnCr-$FcPSO_3$ LDH or GOx/ZnCr-$FcPSO_3$ mixture was spread on the electrode surface and dried in a fridge overnight. Before use, the biosensors were exposed 15 min to saturated glutaraldehyde vapor (25%) to cross-link the entrapped biomolecules. Next, they were soaked in 0.01 M Tris-HCl buffer solution pH 7 for 15 min under stirring to rehydrate the biofilm and remove glutaraldehyde traces.

All experiments were carried out in a sealed cell thermostated at 30 °C with a conventional three-electrode system including an Ag/AgCl reference electrode and a platinum auxiliary electrode. For amperomertic measurement under anaerobic conditions, the sealed cell was maintained under argon atmosphere during the entire experiments and the glucose solution was purged by argon. Before use, the biosensor was then equilibrated into the electrolyte solution at applied potential 0.5 V for 30 min. Injections of glucose solutions were then performed with a syringe. An Autolab 100 potentiostat was used to carry out all the electrochemical experiments.

3. Results and Discussion

3.1. Structural Characterization

Intercalation of anionic sulfonated ferrocene was monitored by X-ray diffraction on sample powders. Hybrid materials display typical PXRD patterns of LDH phases intercalated with organic anions with a series of a high number of (00l) diffraction lines and few (*hk*0) diffraction peaks indicating that their diffraction feature is dominated by the stacking along the perpendicular axis to the layers. The crystallinity of the solids decreases noticeably in the order ZnCr-Cl > ZnCr-$FcPSO_3$ > ZnCr-Fc$(PSO_3)_2$, the hybrid materials exhibiting a strong turbostratic effect due to a low ordering in the interlamellar galleries. This behavior is more pronounced for the ZnCr-Fc$(PSO_3)_2$ LDH phase. The comparison of the size of the crystallographic coherent domains along the *z* axis, reported in Table 1, highlights similar textural properties between the reference material and ZnCr-$FcPSO_3$ with stacked layers ordered along the *c* axis of about 30 nm length while ZnCr-Fc$(PSO_3)_2$ retains an ordered stacking structure not over 5 nm. The scanning electron microscopy images (Fig. 2) reveal, for both hybrid phases, similar aggregates with a large distribution of size made of stuck platelets with undefined shape. However, when dispersed in water under ultrasonic treatment, colloidal solution of ZnCr-$FcPSO_3$ can be obtained with a narrow distribution of size (487 nm) while dissagregation of ZnCr-$(FcPSO_3)_2$ particles was not obtained (1.36 μm average size). Interaction between platelets appears to be stronger for the divalent anion modified LDH than for the hybrid ZnCr-$FcPSO_3$ compound leading to a lower surface area.

The cell parameters (Table 1) are refined from the indexation of the diffraction lines using the hexagonal system with a R-3m symmetry. The expansion of the lamellar structure due to the intercalation of the Fc derivatives is clearly evidenced by the well-defined series of (00l) diffraction lines more particularly for the ZnCr-$FcPSO_3$ phase. Investigation at 2theta values lower than 2° did not show any diffracted signal excluding any higher expansion than that calculated from the observed diffraction data. The basal spacing of the mono and divalent ferrocene LDH derivatives are respectively 2.227(2) nm and 1.869(3) nm. As expected, these values are slightly higher than that found for other anionic ferrocene derivatives which have been intercalated into LDH, i.e., 2.00 nm for ZnCr-$FcSO_3$ or ZnAl-$FcCO_2$, 1.50 nm for ZnCr-Fc$(SO_3)_2$ and 1.55 nm for ZnAl-Fc$(CO_2)_2$ [14, 17].

We have calculated the molecular size for both ferrocene derivatives and their possible configuration within the interlayer space of the LDH (Fig. 3). The resulting theoretical d spacings are compared to the experimental values, showing a good correlation (Table 1). The monosulfonate derivative forms a bilayer stacking associated with water molecules. Due to the low d spacing obtained for the dianion, a tilt orientation in the interlayer space must be envisaged for this molecule, inducing constraints around the ferrocene group.

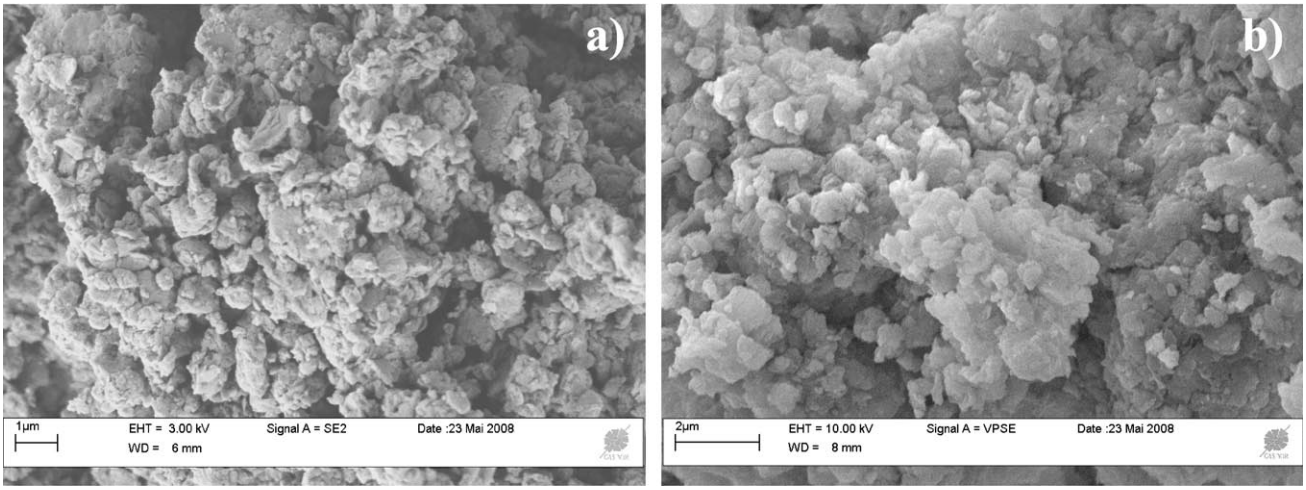

Fig. 2. SEM images of a) Zn_2Cr-$FcPSO_3$ and b) Zn_2Cr-$Fc(PSO_3)_2$ LDH samples at the same magnification ($\times$ 7500).

Table 1. Refined cell parameters and basal spacing of ZnCr-X LDH.

LDH	*a* (nm)	*c* (nm)	*d* (nm)	Size of the cryst. coherent domain (nm)	d_{th} (nm)
ZnCr-Cl	0.31135 (8)	2.316 (1)	0.7721 (2)	30.0	
ZnCr-$FcPSO_3$	0.30770 (8)	6.681 (2)	2.227 (2)	30.0	2.01
ZnCr-$FcP(SO_3)_2$	0.3100 (1)	5.668 (3)	1.889 (3)	4.9	1.91

The presence of organic molecules within the interlayer domain of the LDH structure is confirms by FTIR. The assigned bands of the guest anions are summarized in Table 2. A decrease in the adsorption of νC=O and νO–CO bands was observed for the ZnCr-$Fc(PSO_3)_2$ nanohydrid material. This data suggests a disruption of vibrational modes as a result of the reorientation of the ferrocene moiety due to conformational constraints in the inorganic matrix as suggested by the model (Fig. 3). A similar feature was reported for ferrocenyl alkyl thiols organized in self assembled monolayers [30, 31].

The XPS spectra of the hybrid materials ZnCr-$FcPSO_3$ and ZnCr-$Fc(PSO_3)_2$ shown different Fe2p peak experimental profiles (Fig. 4). Considering some previous results obtained with pure and surface reacted ferrocenes [15, 32], $Fe2p_{3/2}$ component at 708.0 eV can be ascribed to Fe(II) in the ferrocene complex (Table 3). According to the PXRD data, this result can be associated with the $FcPSO_3$ intercalated in the ZnCr LDH matrix. The C1s peak in the case of this sample shows, in the appropriated relative atomic percentages, the different chemical environments of carbon: C–C/C–H at 284.6 eV ($\pi-\pi^*$ shake up satellite of the aromatic cycle at 291.7 eV), C–O at 286.2 eV and O–C=O at 288.7 eV.

The XPS analysis of ZnCr-$Fc(PSO_3)_2$ was more complex with a partial loss of the iron signal (40% decrease relate to ZnCr-$FcPSO_3$). This percentage is quite closed to the theoretical value (50%). Indeed due to the substitution of a monoanion by a dianion, the ZnCr-$FcPSO_3$ sample must contain double amount of iron than the ZnCr-$Fc(PSO_3)_2$ sample (Fig. 3). However, the $Fe2p_{3/2}$ peak (Fig. 4b) has been fitted into two components: on the low energy side (708.2 eV) a small component being attributed to ferrocene dianion inserted into the LDH and a main one arising at higher binding energy (710.2 eV) which is the assignment of iron atoms in a hydroxide environment (Table 3) [33]. The same phenomenon has already been reported by our group for ferrocene sulfonates in LDH, showing the incorporation of some iron atoms in the LDH layers after a possible decomplexation of ferrocene entities [15]. The modification in the layers composition could have undergone through a dissolution-rebuilding of the LDH phase.

Concerning the LDH chemical composition, the examination of Zn3p and Cr2p peaks have confirmed the Zn^{II} and Cr^{III} oxidation states. However a decrease of the Zn/Cr atomic ratio is recorded for ZnCr-$Fc(PSO_3)_2$ (Zn/Cr = 1.62) compared to ZnCr-$FcPSO_3$ (Zn/Cr = 2.20); this seems to be in relation with a + 0.3 eV enhancement of the O1s peak of the LDH layers. Finally, the whole observations done, could indicate a partial replacement of the Zn atoms by some iron atoms in the first top layers (XPS domain of analysis is about 100 nm depth).

3.2. Electrochemical Characterization

In aqueous solution, ferrocene derivatives undergo a one electron oxidation/reduction process:

$$Fc \rightleftharpoons Fc^+ + 1e^-$$

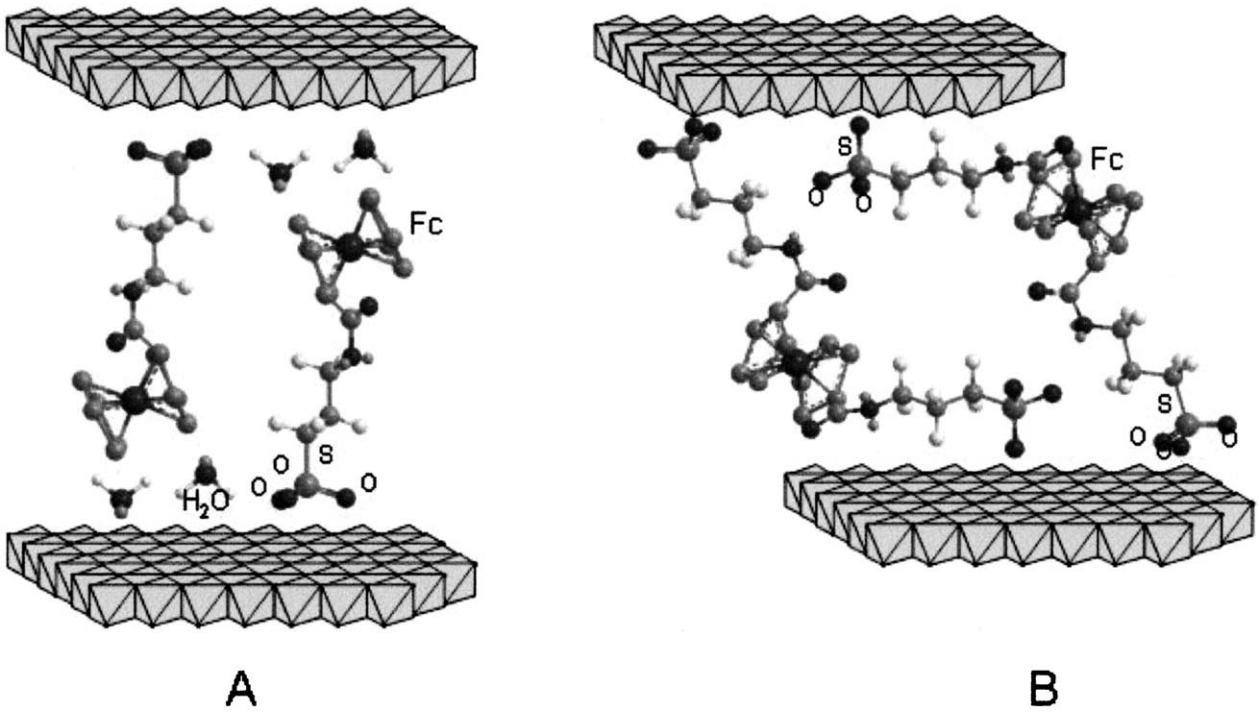

Fig. 3. Schematic representation of ZnCr-$FcPSO_3$ (A) and ZnCr-$Fc(PSO_3)_2$ (B) hybrid materials based on the calculated molecular sizes.

Table 2. Assignment of FTIR vibrations bands of ZnCr-$FcPSO_3$ and ZnCr-$Fc(PSO_3)_2$.

Bands	ZnCr-$FcPSO_3$	Relative intensity	ZnCr-$Fc(PSO_3)_2$	Relative intensity
δCH //,Fc	1003.6	med		
vSO SO_3	1026.7	med	1033.3	med
vSO SO_3	1044.7	int	1043.2	int
vC−C;δCH perp,Fc	1106.3	small	1093.8	small
vO−C−C	1139.2	int	1131.6	small
vSO SO_3	1159.2	int	1160.2	int
vSO SO_3	1173.2	int	1182.7	int
vSO SO_3	1208.2	int	1203.2	int
	1241.8	med	1236.9	med
vC−CO_2	1278.3	int	1275.2	med
			1289.8	med
δCH Fc (subst ring)	1354.9	small	1349.6	small
δCH Fc (subst ring)	1374.4	med	1361.4	small
	1384	med		
vC−C, Fc ring mode	1396	small	1392.4	med
vC−C, Fc ring mode	1413.6	small	1412.9	med
			1442.1	small
δCH_2	1460.4	int		
	1465.2	med		
	1468.8	small		
			1528.6	med
	1566.7	small	1563.8	med
			1651.4	med
			1604.5	med
δHOH	1623.8	int	1629.8	med
	1657.9	small		
v(C=O)	1705.7	int	1705.1	med

Electrochemical reversibility was judged on the basis of peak separation ΔE_p and also on the ratio of anodic to cathodic peak currents (I_{pa}/I_{pc}). In Figures 5 and 6, we compare the cyclic voltammetry curves obtained with the redox species $FcPSO_3$ and $Fc(PSO_3)_2$, in the first case, solubilized in solution using a glassy carbon electrode, and in the second case, when they are intercalated within the LDH interlayer. Table 4 summarizes these CV data. For the ZnCr-

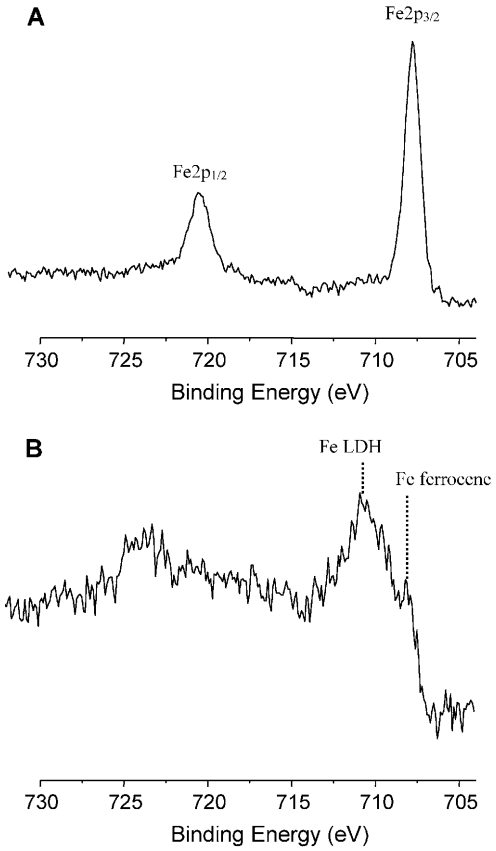

Fig. 4. XPS Fe2p spectra of ZnCr-$FcPSO_3$ (A) and ZnCr-$Fc(PSO_3)_2$ (B).

Table 3. XPS $Fe2p_{3/2}$ binding energies (eV) - FHWM are done into parenthesis with relative intensities.

	ZnCr-$FcPSO_3$	ZnCr-$Fc(PSO_3)_2$
BE $Fe2p_{3/2}$	708.0 eV (1.2)	708.2 eV (2.2) 30% 710.2 eV (2.8) 70%

$FcPSO_3$/GC modified electrode, a slow decrease of the current peak was observed under continuous cycling. A steady state was finally reached after ~20 cycles. The oxidation peak of immobilized $FcPSO_3$ in the LDH interlayer appears at more positive potentials than in aqueous solution. At the same time ΔE_p shows an increase and the ratio (I_{pa}/I_{pc}) decreases (Fig. 5 and Table 4), suggesting that the reversibility of the electrochemical transfer is slowed down when the redox species were intercalated in the LDH matrix. The anodic peak current I_{pa} is proportional to the square root of scan rate ($v^{1/2}$), indicating that the oxidation process of $FcPSO_3$ inside the coating, is under diffusion control.

In a previous study of the electrochemical behavior of ferrocene sulfonates ($FcSO_3$ and $Fc(SO_3)_2$ intercalated in LDH, we have highlighted that the electrochemical transfer occurs via an intracrystallite mechanism in which the diffusion of the electrolyte anions through the hybrid material plays a key role on the reversibility of the electron

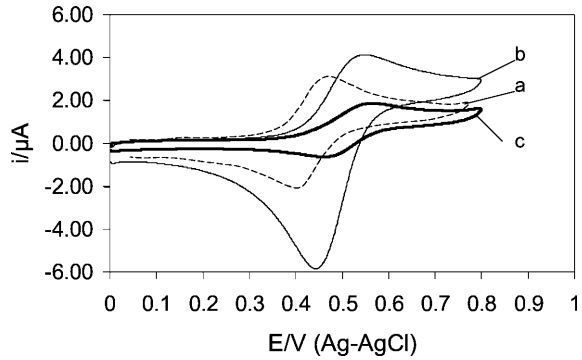

Fig. 5. Cyclic voltammetry of a) 0.5 mM $FcPSO_3$ at GC electrode, b) ZnCr-$FcPSO_3$/GC electrode in 0.1 M $LiClO_4$, c) ZnCr-$FcPSO_3$/GC electrode in 0.01 M TBS pH 7 ($v = 50$ mV/s).

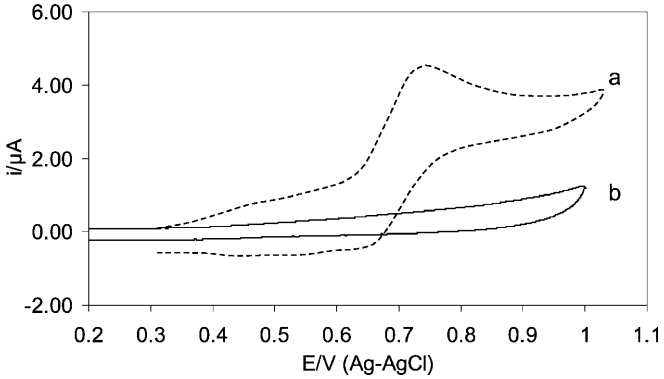

Fig. 6. Cyclic voltammetry of a) 0.5 mM $Fc(PSO_3)_2$ at GC electrode, b) ZnCr-$Fc(PSO_3)_2$/GC electrode in 0.1 M $LiClO_4$, $v = 50$ mV/s.

transfer [14]. In the present case also, the replacement of $LiClO_4$ by a Tris-HCl buffer solution improved the stability and the reversibility of the signal, showing a lower ΔE_p and I_{pa}/I_{pc} tending to 1 (Fig. 5c, Table 4).

For the dianionic derivative $Fc(PSO_3)_2$ in solution , the oxidation potential is shifted toward more positive potential and the reversibility of signal decreases (Fig. 6, Table 4). Moreover, in the case of a glassy carbon electrode modified with a film of ZnCr-$Fc(PSO_3)_2$, the electrochemical signal disappears totally (Fig. 6). This feature can be explained by the XPS and FTIR results. The main part of $Fc(PSO_3)_2$ anion (70%) appears to be decomplexed upon intercalation in the ZnCr LDH structure whereas the remaining ferrocene dianions are immobilized in the LDH interlayer domain with a compacted stacking that should hinder the diffusion of counter anions necessary for the oxidation process. Consequently, the iron atoms present in this sample appear electrochemically silent.

3.3. Glucose Biosensor

With the aim of achieving the appropriate electrical wiring of GOx, we have used the synthetic redox active ZnCr-

Table 4. Electrochemical characteristics of $FcPSO_3$ and $Fc(PSO_3)_2$ in 0.1 M $LiClO_4$.

Compound	E_{pa} (V)	I_{pa} (μA)	ΔE_p (mV)	I_{pa}/I_{pc}
$FcPSO_3$	0.46	3	66	1.1
ZnCr-$FcPSO_3$	0.53	3	88	0.4
ZnCr-$FcPSO_3$[a]	0.55	1	79	9.8
$Fc(PSO_3)_2$	0.74	3	98	1.2
ZnCr-$Fc(PSO_3)_2$	–	–	–	–

[a] in 0.01 M TBS pH 7

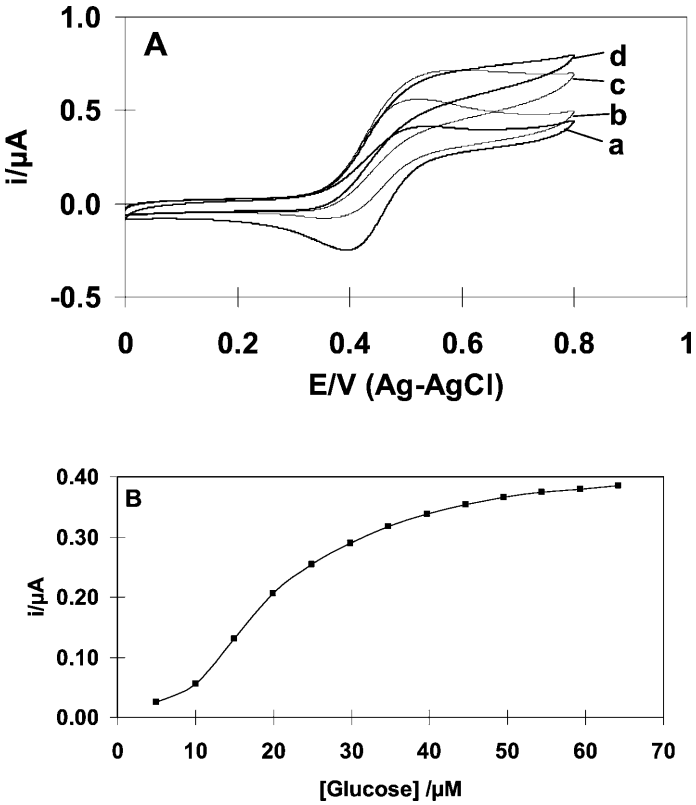

Fig. 7. A) Cyclic voltammetry of GOx/ZnCr-$FcPSO_3$/GC electrode a) in electrolyte, b – d) with successive additions of 2 μmole glucose in 20 mL TBS (0.01 M pH 7 under Ar atmosphere, v = 10 mV/s). B) Glucose calibration curve at GOx/ZnCr-$FcPSO_3$/GC electrode (E_{app} = 0.5 V, 0.01 M TBS pH 7 under Ar at 30 °C).

$FcPSO_3$ LDH as enzyme immobilizing matrix. A glassy carbon electrode was modified by casting a mixture of GOx and ZnCr-$FcPSO_3$ LDH. Different enzyme/LDH ratios have been tested and the electrochemical behavior of the resulting electrodes was investigated by cyclic voltammetry in 0.01 M TBS pH 7. Figure 7A shows the cyclic voltammograms of the enzyme/LDH (80:40 μg) electrode in absence and presence of glucose under anaerobic conditions. The presence of glucose oxidase in the inorganic film caused a drastic decrease of the current intensities of the reversible signal. However, successive additions of glucose between 100 to 300 μM caused an increase of the anodic peak and the concomitant decrease of the cathodic peak. The amount of electroactive $FcPSO_3$ can be evaluated from the charge obtained by integrating the anodic peak at low scan rate (5×10^{-11} mol) and 80 μg of GOx corresponds to 21 U or 4×10^{-10} mol of enzyme (M_{GOx} = 186 kDa). Thus, the described electrocatalytic phenomenon reflects that an efficient electron shuttle from the $FADH_2$ centers in the enzyme to the electrode occurred *via* intercalated $FcPSO_3$.

Since the electrocatalytic current depends on glucose concentration, this bioelectrode device was subsequently tested as an amperometric biosensor for direct determination of glucose. The steady state current was recorded at 0.5 V using a rotating glassy carbon electrode modified with the GOx/ZnCr-$FcPSO_3$ (160:80 μg) coating. The experiments were done using the best enzyme/LDH weight ratio = 2 found in the voltammetry experiments. The resulting calibration curve is shown in Figure 7B. The regression equations relevant to the linear part of the calibration curve between 10 and 25 μM was I(mA) = 13.475 [glucose](M) − 0.0732, R^2 = 0.9905. The calibration curve follows Michaelis – Menten kinetics with an apparent K_M^{app}, evaluated from the electrochemical Linewaever-Burk plot of the calibration curve, equal to 35 μM and I_{max} = 3 μA cm^{-2}. This K_M^{app} value is lower than those reported by Shan et al. for GOx/ZnAl-Cl biosensors using a direct or mediated detection of glucose, 4.4 mM and 2.25 mM, respectively [19, 34]. In order to study the interferent effects of on the response of this mediated GOx biosensor, both concentrations of interferents (ascorbate and urate) and glucose were fixed at 100 μM. The relative responses were 56% and 97% for ascorbate and urate, respectively.

Recently, different glucose biosensors based on the immobilization of glucose oxidase in LDH matrices have been reported in the literature (Table 5) [10, 19, 22, 34 – 36]. Most of the biosensors reported in Table 5 were prepared by the adsorption method, except biosensors 4 and 5. The working electrodes (Pt or glassy carbon electrodes) were modified by casting a mixture of enzyme and LDH. In order to prevent the enzyme leaching, the entrapped biomolecules were cross-linked by a bifunctional agent, the glutaraldehyde in the presence or not of BSA. In biosensor 4, GOx was entrapped within the LDH matrix during its electrogeneration at the Pt electrode [10]. Finally, the sophisticated method developed by Ren et al. for the immobilization of penicillin G acylase [37] was adapted for the covalent grafting of GOx in the interlayer galleries of a LDH by a three step procedure using a glutamate pillared LDH as the starting material (Biosensor 5 in Table 5) [9]. In both last cases, the amount of entrapped enzymes was considerably reduced compared to the adsorption method.

Three transduction processes have been tested. The oxidation of glucose is carried out by the flavin adenine dinucleotide (FAD) component of the glucose oxidase which is converted into $FADH_2$. The latter is reoxidized to the FAD by the dioxygen (a cofactor) with the production of hydrogen peroxide or under anaerobic conditions by mediators. In the first examples, the transduction step corresponded to the electro-oxidation at the underlying Pt

Table 5. Comparison of analytical performance of GOx/LDH biosensors.

Entry	LDH	GOx ($\mu g\ cm^{-2}$)	(U/mg)	Conditions	Electrode	E_{app} (V)	Sensitivity ($mA\ M^{-1}\ cm^{-2}$)	Reference
1	ZnCr-Cl	204	(218)	PBS, O_2	Pt	0.6	19	[35]
2	ZnAl-Cl	204	(218)	PBS, O_2	Pt	0.7	55	[36]
3	ZnAl-Cl	1400	(108)	PBS, O_2	Pt	0.6	35	[34]
4	NiAl-NO_3	46	(179)	PBS, O_2	Pt	0.45	6.2	[10]
5	ZnAl-Glut-GA	0.76	(218)	PBS, O_2	Pt	0.6	0.21	[9]
6	MgAl-$FcSO_3$	107	(179)	PBS, O_2	GC	0.5	2.1	[22]
7	MgAl-$FcCO_2$	107	(179)	PBS, O_2	GC	0.4	4.8	[22]
8	ZnCr-ABTS	102	(218)	PBS, O_2	HRP/GC	0.0	23	[35]
9	FcMeOH/ZnAl-Cl	?-	(108)	PBS, N_2	Pt	0.25	60	[19]
10	ZnCr-$FcPSO_3$	816	(269)	TBS, N_2	GC	0.5	68	[This work]

electrode of the enzymatically generated hydrogen peroxide following the reactions:

$$\text{Glucose} + O_2 \xrightarrow{\text{GOx}} \text{Gluconolactone} + H_2O_2$$

$$H_2O_2 \xrightarrow{\text{Pt}} O_2 + 2H^+ + 2e^-$$

The composition of the LDH matrices seems to influence the biosensor response. In particular, the two first biosensors had the same composition (GOx/LDH 40:40 μg) and the sensitivity of the GOx/ZnCr-Cl biosensor was lower than that obtained with the ZnAl-Cl host matrix. This can be explained by a difference of permeability (Pm) of both membranes. Indeed, Pm of the coatings, in the presence or not of adsorbed GOx, was established using RDE experiments at different rotation rates [9, 36]. It clearly appears that membranes built with ZnCr-Cl LDH exhibited lower permeabilities (2.7×10^{-3} and 4.6×10^{-3} cm s^{-1}) than those obtained with ZnAl-Cl (9×10^{-3} and 2.5×10^{-2} cm s^{-1}). On the other hand, the lower amount of entrapped enzyme reported for the biosensors prepared by electrogeneration of NiAl-NO_3 (9 μg) [10] or by chemical grafting in ZnAl-Gu-GA (0.15 μg) can explain, at least partially, their lower sensitivity values.

The second transduction processes were based on the electrocatalytic detection of hydrogen peroxide using either redox mediators (biosensors 6 and 7 in Table 5) [22] or a bienzymatic electrode composed of GOx and horseradish peroxidase (HRP) (biosensor 8 in Table 5) [35]. In all cases, the anionic mediators, ferrocene sulfonate ($FcSO_3$) or carboxylate ($FcCO_2$) and 2,2′-azinobis 3-ethylbenzothiazoline-6-sulfonate (ABTS), were intercalated in the LDH interlayer domains. Yang and Mu have reported that polyaniline doped with $FcSO_3$ can effectively catalyze the oxidation of H_2O_2 [38]. The same feature was observed when ferrocene sulfonates were immobilized in a LDH host structure (Fig. 8A). Recently, Colombari et al. have exploited the mediated oxidation of H_2O_2 by ferrocene anions ($FcSO_3$ and $FcCO_2$) as transduction steps in their GOx/MgAl LDH biosensors [22]. However, the sensitivities remain low (2–5 mA M^{-1} cm^{-2}). With the bienzymatic GOx-HRP/ZnCr-ABTS modified electrode, hydrogen peroxide produced in the first GOx reaction is detected with the HRP/ZnCr-ABTS system [35]. The electroactive anions ABTS play the role of electron shuttle between the redox center of HRP and the electrode. The electrochemical transduction step corresponds to the reduction at 0.0 V of $ABTS^{+\cdot}$ enzymatically formed in the presence of H_2O_2. The resulting bienzymatic configuration appeared to be very sensitive to glucose and the low applied potential prevented any possible oxidation of ascorbate and urate.

Finally, glucose determination can be performed under anaerobic condition where $FADH_2$ was reoxidized to the FAD by ferricinium (Fc^+) derivatives, followed by the reoxidation of Fc to Fc^+ directly at the electrode. Few years ago, Calvo and coll. have reported that ferrocene sulfonates in solution are efficient electron mediators in this redox enzyme catalysis [39, 40]. However, it is not true when ferrocene sulfonates were immobilized in LDH. As observed in cyclic voltammetry, the presence of GOx in the coating caused a drastic decrease of the current intensities at the GOx/ZnCr-$FcSO_3$ (Fig. 8B) or GOx/ZnCr-$Fc(SO_3)_2$ (curve not shown) modified electrodes and moreover no electrocatalytic current was observed in the presence of glucose under anaerobic condition. The same conclusion was deduced from the amperometric experiments performed with the GOx/MgAl-$FcCO_2$ biomembrane [22]. Other ferrocene derivatives have been therefore tested (biosensors 9 and 10 in Table 4). In the present paper, we have used (3-sulfopropyl)ferrocene-carboxylate instead of ferrocene sulfonates. In this case, we have shown that an efficient electron shuttle between the enzyme and the electrode occurred via intercalated $FcPSO_3$, given the highest sensitivity (Table 5). Although the mechanism of electron transfer is not completely established, it appears that the presence of the alkyl chain linked to the ferrocene group enhanced the efficiency of the electrocatalytic process since no mediated process was observed with intercalated $FcSO_3$ or $FcCO_2$ where there is no linker between the ferrocene and the anionic group in interaction with the hydroxide layers of the LDH.

Alternatively, ferrocene-methanol (FcMOH), a neutral molecule, was simply adsorbed on the external phase of the ZnAl-Cl LDH particles [19]. This biosensor configuration

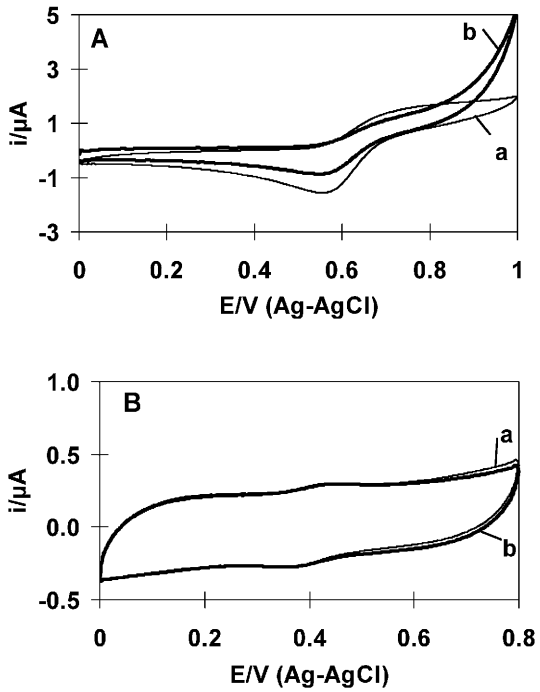

Fig. 8. A) Cyclic voltammetry of ZnCr-Fc$(SO_3)_2$/GC electrode a) in electrolyte, in the presence 5 mM of H_2O_2 (TBS 0.01 M pH 7, $v = 50$ mV/s). B) Cyclic voltammetry of GOx/ZnCr-FcSO_3/GC electrode a) in electrolyte, in the presence 250 μM glucose (0.1 M PBS M pH 5, $v = 50$ mV/s).

allowed the detection of glucose at 0.25 V, with a dramatically reduced interference of easily oxidizable interferents. However, these authors did not report on the operational or storage stability of their mediated biosensor. In the case the GOx/ZnCr-FcPSO_3 electrode, two successive measurements gave the same sensitivity, however this electrode presented only 50% of its initial response after four days in solution at 4 °C. Other biosensors, working under aerobic conditions, present better storage stabilities. Their responses remained unchanged for at least ten days, afterwards their responses decreased slowly to reach 70% after 18 days [11] or 62% after 30 days [34].

4. Conclusions

The number of publications on biosensors based on LDH as immobilization matrix is limited in comparison with that reported for entrapment of enzymes in sol-gel made host matrices, for instance. However, the versatility of LDH compositions and of their physical properties allows the immobilization of enzymes, such as glucose oxidase with a good biocompatibility. Moreover, the possible co-immobilization of adequate redox mediators in the interlayer domains of LDH allows the mediated detection of the substrates or the regeneration of the enzyme active site. In conclusion, the results presented therein confirm that the synthesis a new LDH nanohybrid materials with specific textural and electrochemical properties will certainly open new routes for the biosensor development.

5. References

[1] L. He, C.-S. Toh, *Anal. Chim. Acta* **2006**, *556*, 1.
[2] A. Walcarius, *Chem. Mater.* **2001**, *13*, 3351.
[3] A. Walcarius, *Electroanalysis* **2008**, *20*, 711.
[4] C. Mousty, *Appl. Clay Sci.* **2004**, *27*, 159.
[5] E. Ruiz-Hitzky, in *Organic-Inorganic Materials: From Intercalation Chemistry to Devices* (Ed. Gomez-Romero), Wiley-VCH, Weinheim **2004**, pp. 15.
[6] I. K. Aamir, D. O'Hare, *J. Mater. Chem.* **2002**, *12*, 3191.
[7] J.-H. Choy, S.-J. Choi, O. Jae-Min, P. Taeun, *Appl. Clay Sci.* **2007**, *36*, 122.
[8] C. Forano, V. Prévot in *Enzyme-based Bioinorgnaic Materials* (Eds: E. Ruiz-Hitzky, K. Ariga, Y. Lvov), Wiley-VCH **2008**, pp. 443.
[9] C. Forano, S. Vial, C. Mousty, *Curr. NanoSci.* **2006**, *2*, 283.
[10] A. Mignani, G. Luciono, S. Lanteri, R. Leardi, E. Scavetta, D. Tonelli, *Anal. Chim. Acta* **2007**, *599*, 36.
[11] A. Mignani, E. Scavetta, D. Tonelli, *Anal. Chim. Acta* **2006**, *577*, 98.
[12] C. Mousty, S. Therias, C. Forano, J.-P. Besse, *J. Electroanal. Chem.* **1994**, *374*, 63.
[13] S. Therias, C. Mousty, C. Forano, J. P. Besse, *Langmuir* **1996**, *12*, 4914.
[14] S. Therias, B. Lacroix, B. Schollhorn, C. Mousty, P. Palvadeau, *J. Electroanal. Chem.* **1998**, *454*, 91.
[15] S. Morlat-Therias, C. Mousty, P. Palvadeau, P. Molinie, P. Leone, J. Rouxel, C. Taviot-Gueho, A. Ennaqui, A. de Roy, J. P. Besse, *J. Solid State Chem.* **1999**, *144*, 143.
[16] P. Wang, G. Zhu, *Electrochem. Commun.* **2002**, *4*, 36.
[17] S. Gago, M. Pillinger, T. M. Santos, J. Rocha, I. S. Goncalves, *Eur. J. Inorg. Chem.* **2004**, 1389.
[18] L. Mohanambe, S. Vasudevan, *Inorg. Chem.* **2005**, *44*, 2128.
[19] D. Shan, W. Yao, H. Xue, *Biosens. Bioelectron.* **2007**, *23*, 432.
[20] L. Fernandez, H. Carrero, *Electrochim. Acta* **2005**, *50*, 1233.
[21] I. Ledezma, L. Fernandez, *Revista Tecnica de la Facultad de Ingeniera* **2007**, *30*, 234.
[22] M. Colombari, B. Ballarin, I. Carpani, L. Guadagnini, A. Mignani, E. Scavetta, D. Tonelli, *Electroanalysis* **2007**, *19*, 2321.
[23] A. Chaubey, B. D. Malhotra, *Biosens. Bioelectron.* **2002**, *17*, 441.
[24] M. P. Garcia Armada, J. Losada, F. J. Lopez-Villanueva, H. Frey, B. Alonso, C. M. Casado, *J. Organomet. Chem.* **2008**, *693*, 2803.
[25] V. S. Tripathi, V. B. Kandimalla, H. Ju, *Sens. Actuators, B* **2006**, *114*, 1071.
[26] B. Ballarin, M. C. Cassani, R. Mazzoni, E. Scavetta, D. Tonelli, *Biosens. Bioelectron.* **2007**, *22*, 1317.
[27] B. A. Milagres, L. T. Kubota, G. de OliveiroNeto, *Electroanalysis* **1996**, *9*, 489.
[28] C. Tsiafoulis, A. B. Florou, P. Trikalitis, N., T. Bakas, M. I. Prodromidis, *Electrochem. Commun.* **2005**, *7*, 781.
[29] J. H. Helberger, G. Manecke, R. Heyden, *Liebigs Ann. Chem.* **1949**, *565*, 22.
[30] D. D. Popenoe, R. S. Deinhammer, M. D. Porter, *Langmuir* **1992**, *8*, 2521.
[31] A. S. Viana, A. H. Jones, L. M. Abrantes, M. Kalaji, *J. Electroanal. Chem.* **2001**, *500*, 290.
[32] R. Zanoni, F. Cattaruzza, C. Coluzza, E. A. Dalchiele, F. F. Decker, G. Di Santo, A. Flamini, L. Funari, A. G. Marrani, *Surf. Sci.* **2005**, *575*, 260.

[33] G. Bhargava, I. Gouzman, C. M. Chun, T. A. Ramanaryann, S. L. Bernasek, *Appl. Surf. Sci.* **2007**, *253*, 4322.
[34] D. Shan, W. Yao, H. Xue, *Electroanalysis* **2006**, *18*, 1485.
[35] D. Shan, S. Cosnier, C. Mousty, *Anal. Lett.* **2003**, *36*, 909.
[36] S. Cosnier, C. Mousty, C. Gondran, A. Lepellec, *Mater. Sci. Eng. C* **2006**, *26*, 442.
[37] L. Ren, J. He, S. Zhang, D. G. Evans, X. Duan, *J. Mol. Catal. B, Enzymatic* **2002**, *18*, 3.
[38] Y. Yang, S. Mu, *Biosens. Bioelectron.* **2005**, *21*, 74.
[39] E. Liaudet, F. Battaglini, E. J. Calvo, *J. Electroanal. Chem.* **1990**, *293*, 55.
[40] F. Battaglini, E. J. Calvo, *J. Chem. Soc. Faraday Trans.* **1994**, *90*, 978.

